

Single event burnout in SiC MOSFETs induced by nuclear reactions with high-energy oxygen ions

Shi-Wei Zhao(赵世伟), Bing Ye(叶兵), Yu-Zhu Liu(刘郁竹), Xiao-Yu Yan(闫晓宇), Pei-Pei Hu(胡培培), Teng Zhang(张腾), Peng-Fei Zhai(翟鹏飞), Jing-Lai Duan(段敬来), Jie Liu(刘杰)
Citation: Chin. Phys. B, 2025, 34 (**7**): 078501. DOI: 10.1088/1674-1056/adcd45
http://cpb.iphy.ac.cn; http://iopscience.iop.org/cpb

What follows is a list of articles you may be interested in

Single event effects evaluation on convolution neural network in Xilinx 28 nm system on chip

Xu Zhao(赵旭), Xuecheng Du(杜雪成), Xu Xiong(熊旭), Chao Ma(马超), Weitao Yang(杨卫涛), Bo Zheng(郑波), and Chao Zhou(周超)
Chin. Phys. B, 2024, 33 (**7**): 078501. DOI: 10.1088/1674-1056/ad3b82

Experiment and simulation on degradation and burnout mechanisms of SiC MOSFET under heavy ion irradiation

Hong Zhang(张鸿), Hongxia Guo(郭红霞), Zhifeng Lei(雷志锋), Chao Peng(彭超), Zhangang Zhang(张战刚), Ziwen Chen(陈资文), Changhao Sun(孙常皓), Yujuan He(何玉娟), Fengqi Zhang(张凤祁), Xiaoyu Pan(潘霄宇), Xiangli Zhong(钟向丽), and Xiaoping Ouyang(欧阳晓平)
Chin. Phys. B, 2023, 32 (**2**): 028504. DOI: 10.1088/1674-1056/ac8cda

Sensitivity of heavy-ion-induced single event burnout in SiC MOSFET

Hong Zhang(张鸿), Hong-Xia Guo(郭红霞), Feng-Qi Zhang(张凤祁), Xiao-Yu Pan(潘霄宇), Yi-Tian Liu(柳奕天), Zhao-Qiao Gu(顾朝桥), An-An Ju(琚安安), and Xiao-Ping Ouyang(欧阳晓平)
Chin. Phys. B, 2022, 31 (**1**): 018501. DOI: 10.1088/1674-1056/ac051d

Influences of supply voltage on single event upsets and multiple-cell upsets in nanometer SRAM across a wide linear energy transfer range

Yin-Yong Luo(罗尹虹), Wei Chen(陈伟), Feng-Qi Zhang(张凤祁), and Tan Wang(王坦)
Chin. Phys. B, 2021, 30 (**4**): 048502. DOI: 10.1088/1674-1056/abcf38

Investigation of single event effect in 28-nm system-on-chip with multi patterns

Wei-Tao Yang(杨卫涛), Yong-Hong Li(李永宏)†, Ya-Xin Guo(郭亚鑫), Hao-Yu Zhao(赵浩昱), Yang Li(李洋), Pei Li(李培), Chao-Hui He(贺朝会), Gang Guo(郭刚), Jie Liu(刘杰), Sheng-Sheng Yang(杨生胜), and Heng An(安恒)
Chin. Phys. B, 2020, 29 (**10**): 108504. DOI: 10.1088/1674-1056/ab99b8

Single event burnout in SiC MOSFETs induced by nuclear reactions with high-energy oxygen ions

Shi-Wei Zhao(赵世伟)[1,2], Bing Ye(叶兵)[1,2,3], Yu-Zhu Liu(刘郁竹)[1,2], Xiao-Yu Yan(闫晓宇)[1], Pei-Pei Hu(胡培培)[1], Teng Zhang(张腾)[4], Peng-Fei Zhai(翟鹏飞)[1,2,3], Jing-Lai Duan(段敬来)[1,2,3], and Jie Liu(刘杰)[1,2,3,†]

[1] *Institute of Modern Physics, Chinese Academy of Sciences (CAS), Lanzhou* 730000, *China*
[2] *School of Nuclear Science and Technology, University of Chinese Academy of Sciences, Beijing* 100049, *China*
[3] *State Key Laboratory of Heavy Ion Science and Technology, Institute of Modern Physics, Chinese Academy of Sciences (CAS), Lanzhou* 730000, *China*
[4] *Nanjing Electronic Devices Institute, Nanjing* 210016, *China*

(Received 2 March 2025; revised manuscript received 13 April 2025; accepted manuscript online 16 April 2025)

We investigate the impact of high-energy O ions on the occurrence of single-event burnout (SEB) in silicon carbide (SiC) metal–oxide–semiconductor field-effect transistors (MOSFETs) under various bias conditions. Through a combination of SRIM, GEANT4, and TCAD simulations, we explore the role of secondary ions generated by nuclear reactions between high-energy O ions and SiC materials. These secondary ions, with significantly higher linear energy transfer (LET) values, contribute to electron–hole pair generation, leading to SEB. Our results show that the energy deposition and penetration depth of these secondary ions, especially those with high LET, are sufficient to induce catastrophic SEB in SiC MOSFETs. The study also highlights the critical influence of reverse bias voltage on SEB occurrence and provides insights into the failure mechanisms induced by nuclear reactions with high-energy O ions. This work offers valuable understanding for improving the radiation resistance of SiC-based power devices used in space and high-radiation environments, contributing to the design of more reliable electronics for future space missions.

Keywords: heavy ion, silicon carbide metal–oxide–semiconductor field-effect transistor (SiC MOSFET), nuclear reactions, single-event burnout (SEB)

PACS: 85.30.Tv, 61.80.Jh, 51.50.+v, 84.30.Jc

DOI: 10.1088/1674-1056/adcd45 **CSTR:** 32038.14.CPB.adcd45

1. Introduction

Silicon carbide (SiC), as a third-generation wide bandgap semiconductor material, has garnered significant attention for its advantages such as a wide bandgap, high thermal conductivity, and high electron mobility.[1] These properties have made SiC widely used in high-voltage power semiconductor devices. Under the same rated voltage conditions, SiC power devices are only about one-tenth the volume of their silicon counterparts. With these performance advantages, SiC power devices have become highly anticipated for space applications, where there are stringent requirements for weight and size of electronic components.[2,3] While previous studies have shown that SiC power devices have strong resistance to total ionizing dose (TID) effects and displacement damage (DD), the sensitivity to single-event effects (SEEs) remains a critical limitation for the application of SiC power devices in space radiation environments.[4–7] Space radiation, which primarily comes from galactic cosmic rays (GCRs) and solar energetic ions (SEPs), contains high-energy protons and heavy ions, both of which induce SEEs in spacecraft electronics. High-energy protons and heavy ions in space are known to cause single-event burnout (SEB) in power semiconductor devices, representing a significant risk to the safe operation of spacecraft in orbit.[8,9]

In ground-based accelerator studies of single-ion effects on SiC power devices, most irradiation experiments employ high linear energy transfer (LET) heavy ions (such as LET $>$ 37 or 75 MeV·cm^2·mg^{-1}) to explore the failure mechanisms of SiC power devices under single-ion effects.[10] Existing research results detail several SEEs observed in SiC power metal–oxide–semiconductor field-effect transistors (MOSFETs) exposed to heavy ions with varying LETs, including latent gate damage, single-event leakage current (SELC), and SEB. All evaluated MOSFETs exhibited latent damage to the gate oxide from ions with LET greater than approximately 10 MeV·cm^2·mg^{-1}. Irradiation at higher drain–source voltages can lead to an increase in I_{DG} that is measurable during the ion beam run. The I_{DG} leakage degradation mode is less prominent under irradiation with lower LET. At still higher V_{DS}, all tested devices showed increasing I_{DS} leakage degradation. This can result in the degradation of the breakdown voltage and an increase in the off-state drain leakage current. The threshold voltage for this type of SELC was found to be a LET of about $>$ 10 MeV·cm^2·mg^{-1}.[11] However, heavy ions in GCRs span a range of elements from low to high atomic numbers. Low-Z ions, such as O, although having a lower

†Corresponding author. E-mail: j.liu@impcas.ac.cn

© 2025 Chinese Physical Society and IOP Publishing Ltd. All rights, including for text and data mining, AI training, and similar technologies, are reserved.

LET in device materials, are prevalent in GCRs and are difficult to directly induce device failure. However, high-energy O ions can generate high-energy secondary ions through nuclear reactions. These secondary ions, with higher LET, can excite a large number of electron–hole pairs in the material.[12]

Existing research has primarily focused on high-energy protons and atmospheric neutrons interacting with the SiC lattice, generating secondary ions that can induce SEB in SiC MOSFETs and diodes.[13–16] Earlier studies have also detected SEB in Si-based power MOSFETs caused by nuclear reactions between incident heavy ions. Experiments using ions like 520 MeV Kr and 3536 MeV Xe have shown significantly different SEB threshold voltages despite having similar LET values. Further analysis reveals that Xe ions, due to nuclear reactions with Si atoms, generate excess charge, leading to a lower SEB threshold. These results suggest that for high-voltage devices with larger sensitive volumes, traditional LET-based SEB threshold testing may be insufficient.[17] However, there is a lack of experimental research and mechanism regarding the SEB induced in SiC MOSFETs by low-LET, high-energy heavy ion nuclear reactions. Research into the effects of high-energy O ions provides a more realistic simulation of radiation effects for SiC power devices in space environments. Therefore, studying the SEB degradation process and failure mechanisms of SiC MOSFETs induced by nuclear reactions with high-energy O ions is crucial.

In this work, we investigate the effects of high-energy O ions ($^{18}O^{6+}$) on the off-state SiC MOSFETs. The differences in the irradiation response of the devices under different biasing conditions are analyzed. Using SRIM and GEANT4 simulations, we find that secondary ions generated during nuclear reactions between the incident O ions and the device materials have sufficient range to penetrate the entire epitaxial layer of the SiC MOSFET. This range is one of the key parameters in understanding SEEs in SiC MOSFETs. Further TCAD simulations show that secondary ions with LET > 10 MeV·cm^2·mg^{-1}, produced by high-energy O ions, are sufficient to induce SEB in the device. This study provides a deeper understanding of the role of secondary ions in the SEB process and offers insights into improving the radiation resistance of SiC-based power devices used in space and high-radiation environments.

2. Experiment setup and results

The device under test (DUT) used in this study was provided by the Nanjing Institute of Electronic Devices. Specifically, the DUTs are SiC MOSFETs with rated parameters of 1200 V–15 A. Figure 1(a) shows the physical picture of the SiC MOSFET after removing the epoxy resin packaging layer from the device surface, and Fig. 1(b) presents the cross-sectional scanning electron microscopy (SEM) image of the DUT.

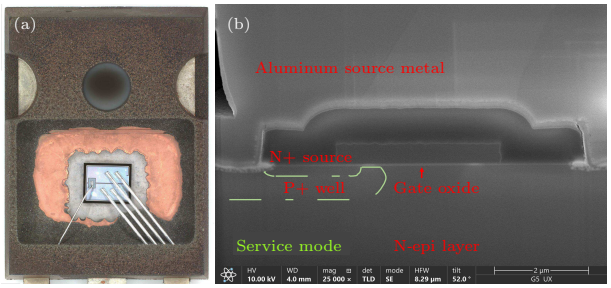


Fig. 1. (a) Physical picture of the SiC MOSFET. (b) Cross-sectional SEM image of the DUT.

Heavy ion irradiation experiments were conducted at the Heavy Ion Research Facility in Lanzhou (HIRFL), located within the Institute of Modern Physics, Chinese Academy of Sciences, in the High Energy Radiation Effects experimental terminal (HERE). In this study, high-energy O ions with an initial energy of 60 MeV/u were used. The residual energy when the O ions reached the DUT surface was 1033.25 MeV. The LET of the O ions at the device surface was 0.59 MeV·cm^2·mg^{-1}, and the range of the O ions in the SiC material was calculated to be 4.71 mm using the SRIM 2013 software.[18] The experiment was conducted under atmospheric conditions and at room temperature ($\sim$ 298 K).

During the heavy ion irradiation experiment, the Keithley 2651A and Keithley 2657A power supplies were used to monitor and record the gate leakage current (I_{GS}) and drain leakage current (I_{DS}), respectively. To ensure that the DUT was in the off-state and to make it most sensitive to heavy ion radiation, the SiC MOSFET devices were biased with the gate and source grounded (0 V), while 650 V and 700 V reverse bias voltages (V_{DS}) were applied to the drain during irradiation.

During irradiation experiments, the process was terminated when the cumulative ion fluence reached 1×10^5 ions·cm^{-2} or when the device leakage current exceeded the preset current limit (10 mA). The ion flux was maintained at approximately 1000 ions·cm^{-2}·s^{-2} throughout the irradiation period. To minimize the impact of device-to-device variability, two sets of repeated experiments were conducted under each bias condition. Figure 2 shows the results of I_{DS} for the device as a function of the irradiation time (ion fluence). The I_{DS} of both DUTs increased periodically with the pulse of the O ion beam and rapidly returned to the pre-irradiation state once the beam was stopped. No degradation in electrical performance was observed for the device under 650 V reverse bias.

However, when the reverse bias voltage was increased to 700 V, catastrophic SEB occurred in both devices under O ion irradiation. Figure 3 presents the I_{DS} results for the devices under 650 V and 700 V bias conditions. When the I_{DS} reached 10 mA, it indicated that the device had experienced

SEB. These experimental results highlight that the reverse bias voltage during O ion irradiation is a critical factor in the catastrophic failure of SiC MOSFETs. SEB occurs only when the bias voltage exceeds a certain threshold, which aligns with findings reported in the literature.[19]

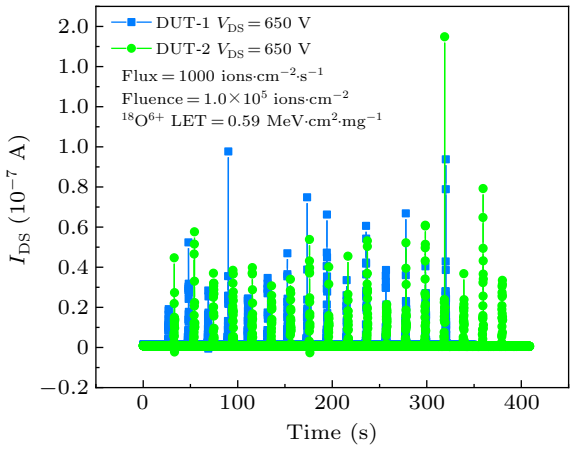


Fig. 2. The I_{DS} responses of O ions irradiated DUTs under 650 V bias.

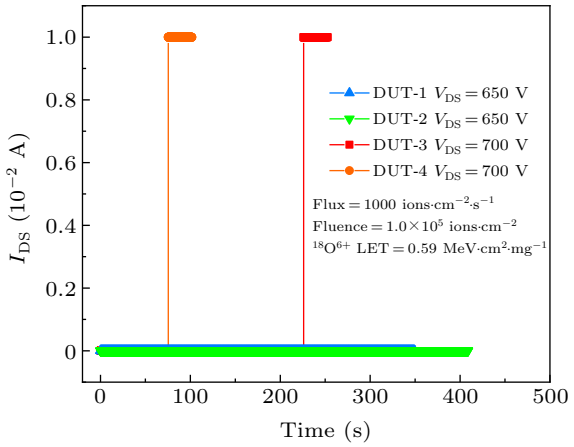


Fig. 3. The I_{DS} responses of O ions irradiated DUTs under 650 V and 700 V bias.

High-energy heavy ions incident on SiC MOSFETs interact with the device materials through both ionization processes and nuclear reaction processes. High-energy ions transfer energy to electrons in the material through direct collisions, causing excitation or ionization of the material's electrons. The nuclear reaction process involves collisions between heavy ions and atomic nuclei in the device material, which results in the generation of secondary ions.

According to the SRIM software calculations, the LET value of the 1033.25 MeV O ions in SiC material is only 0.59 MeV·cm^2·mg^{-1}, which is insufficient to directly trigger SEB in the DUTs.[20] Therefore, we conclude that the SEB observed in the SiC MOSFETs in this experiment is highly possibly caused by the ionization effects of secondary ions, which are generated through nuclear reactions between high-energy O ions and the device materials.

3. Simulations and results

The combination of GEANT4 and TCAD simulations plays a crucial role in understanding the SEB phenomenon in SiC MOSFETs, especially when induced by secondary ions generated through nuclear reactions between high-energy O ions and device materials. GEANT4 is an advanced simulation toolkit for ion transport and interaction, providing a detailed model of how high-energy ions interact with the SiC material, including secondary ion generation.[21,22] This helps in accurately characterizing the secondary ions' energy spectra and LET profiles, which are critical in predicting their potential to induce SEB. On the other hand, TCAD simulations offer a powerful tool for modeling the electrical behavior of the device, particularly in understanding how the generated secondary ions induce electronic excitations and carrier generation in the device's active layers.[5] By integrating both simulations, we can obtain a comprehensive view of the physical and electrical processes that lead to SEB, allowing for more accurate predictions of device behavior under space radiation environments.

3.1. GEANT4 simulation and results

Using GEANT4 software, we simulated the secondary ions generated by the incident 1033.25 MeV O ions on a SiC MOSFET device. This simulation provided detailed insights into the interaction mechanisms between the high-energy O ions and the materials that make up the device. Figure 4 illustrates the various material layers within the SiC MOSFET through which the O ions pass. These interactions are particularly critical in the induction of SEEs, especially SEB, in power semiconductor devices.

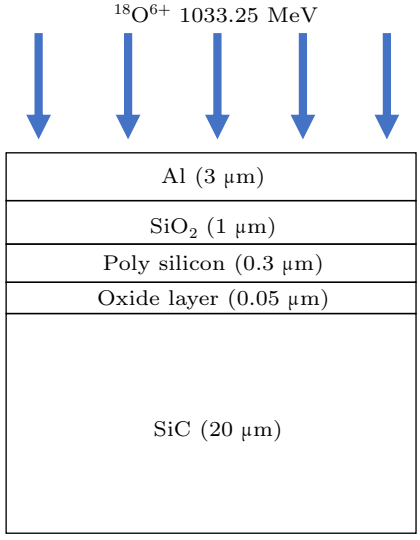


Fig. 4. GEANT4 simulation of a SiC MOSFET device model.

To accurately model the nuclear reactions caused by the incident O ions, we utilized the G4IonINCLXXPhysics and

G4HadronInelasticQBBC models, which are designed to handle the nuclear interactions between high-energy heavy ions and the atomic nuclei in the device material. These models are particularly adept at simulating inelastic hadron interactions and the nuclear reactions that generate secondary ions such as protons, neutrons, and lighter ions. The G4IonINCLXXPhysics model, specifically tailored for heavy ions, simulates the interactions of the incident ion with the target material, while the G4HadronInelasticQBBC model accounts for the interaction of secondary heavy ions with the material, providing a more comprehensive view of the nuclear processes at play.[21]

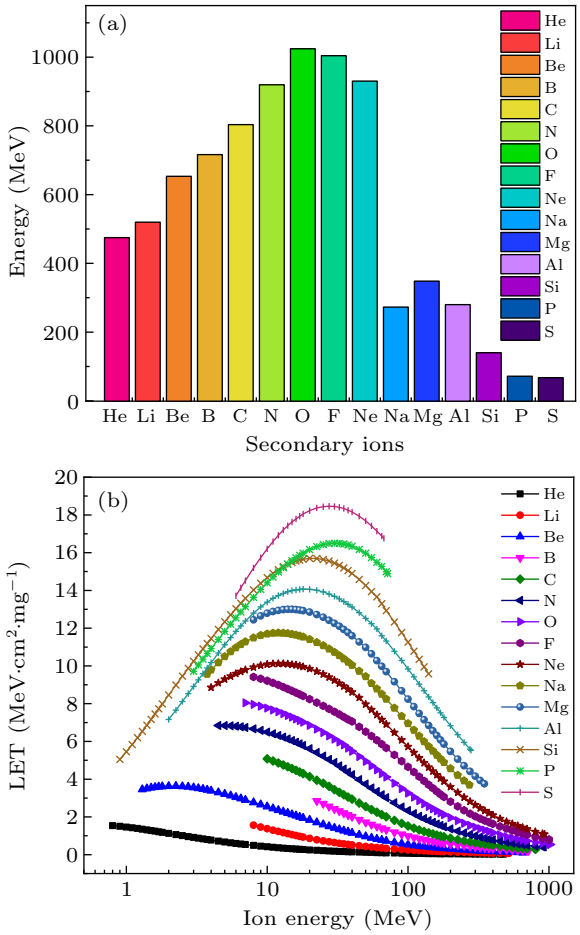


Fig. 5. (a) Energy distribution of secondary ions. (b) LET distributions of secondary ions.

The secondary ions induced by the O ions' interaction with the SiC MOSFET materials include a range of elements, specifically ions with atomic numbers between 2 (helium) and 16 (sulfur). With regard to these secondary ions, it is highly likely that the electron–hole pairs generated through direct ionization lead to the occurrence of SEB, and contribute significantly to the overall ionization and carrier generation within the device. The energy distribution of these secondary ions, depicted in Fig. 5(a), reveals a broad range of energies, which influence the extent of damage they can cause in the device. Figure 5(b) shows the LET distribution of these secondary ions within the SiC material, illustrating the varying degrees of energy deposition that occur as the secondary ions propagate through the device. The LET is a critical factor in determining the potential of these secondary ions to induce damage.

There is a significant variation in the LET values among different secondary ions. The range and LET distribution of secondary ions (such as Na to S) in the SiC material were calculated using SRIM and are shown in Fig. 6.

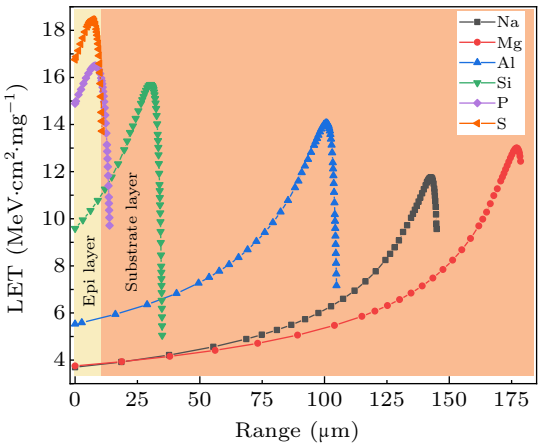


Fig. 6. Range and LET distribution of secondary ions in SiC material.

Ions such as He to Ne have LET values below 1 MeV·cm^2·mg^{-1}, which are insufficient to trigger SEB in the device. However, ions like Si, P, and S exhibit much higher LET values, all exceeding 8 MeV·cm^2·mg^{-1}, and their range is sufficient to penetrate the entire epitaxial layer of the device. These high LET ions are more likely to induce SEB in SiC MOSFETs.

3.2. TCAD simulation and results

The high-energy O ion irradiation experiments reveal that catastrophic SEB occurs in SiC MOSFETs when the drain bias voltage exceeds a critical threshold. GEANT4 and SRIM simulation results demonstrate that the secondary ions generated via nuclear reactions possess sufficient range to penetrate the device's epitaxial layer. To further elucidate the mechanism by which secondary ions influence SEB, the effect of their LET was investigated using TCAD modeling.

The device structure is depicted in Fig. 7, while Table 1 provides a comprehensive description of the simulation parameters employed.

Table 1. The device parameters used in the simulation.

Parameters	Unit	Values
P region width (W)	μm	3.0
P region depth (X_j)	μm	1.0
N$^-$ epi layer thickness (T_{epi})	μm	10.0
Epi buffer layer thickness (T_{buffer})	μm	0.8
N$^+$ substrate thickness (T_{sub})	μm	2.0
Gate oxide thickness (T_{OX})	μm	0.05

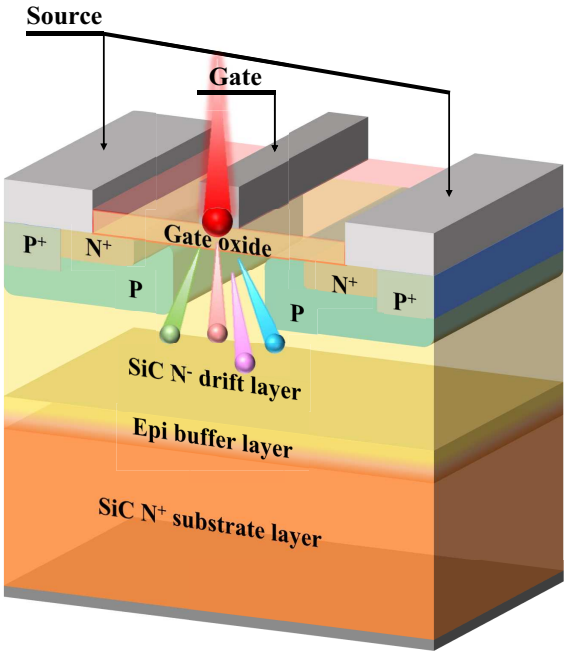


Fig. 7. SiC MOSFET cell structure.

The 3D-TCAD simulator was used to construct the device model, which includes a 10 μm epitaxial layer and a 2 μm substrate. As shown in Fig. 7, a 0.5–1 μm buffer layer was introduced during the device manufacturing process to mitigate the propagation of defects from the substrate to the epitaxial layer. Consequently, the simulation model incorporated the actual process parameters, including a 0.8 μm epitaxial buffer layer between the epitaxial layer and the substrate. The simulation integrated several physical models, including band structure and carrier models, mobility models, carrier recombination models (such as Auger recombination and impact ionization), Shockley–Read–Hall (SRH) recombination, and thermodynamic models. Additionally, a heavy-ion model was used to simulate the transient behavior of heavy ions upon incidence.

Six different LET values of secondary ions were chosen to explore the SEB threshold induced by secondary ions. The specific parameters are listed in Table 2.

Table 2. The device parameters used in the simulation.

Parameters	Unit	Values
LET_1	MeV·cm^2·mg^{-1}	1.1
LET_2	MeV·cm^2·mg^{-1}	3.7
LET_3	MeV·cm^2·mg^{-1}	5.5
LET_4	MeV·cm^2·mg^{-1}	9.9
LET_5	MeV·cm^2·mg^{-1}	14.8
LET_6	MeV·cm^2·mg^{-1}	16.7

The spatial distribution of the current density helps to elucidate how the ion-induced currents can lead to localized heating and potential failure mechanisms, such as SEB. By presenting these simulation results, we aim to provide a clearer understanding of how current density variations following ion impact affect the overall reliability and performance of the device.

The electric field of the epitaxial layer at a bias voltage of 700 V influences the behavior of the electron–hole pairs generated by ion incidence. Due to the shutdown state of the device, the electric field causes these charge carriers to be collected, resulting in a high current density peak along the ion incident path. Figure 8 shows the spatial distribution of the total current density within the device, illustrating how the current density evolves as a function of depth after ion impact.

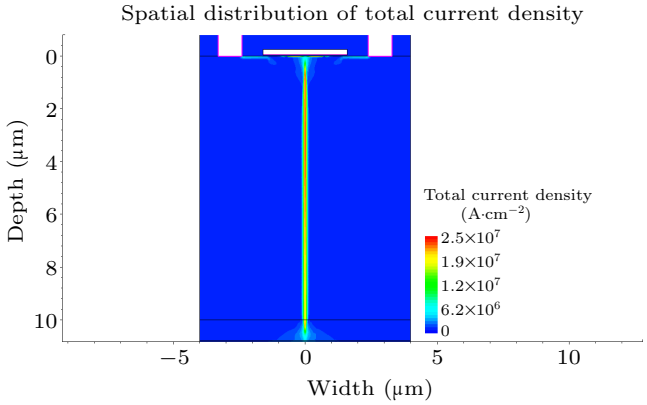


Fig. 8. Spatial distribution of the total current density.

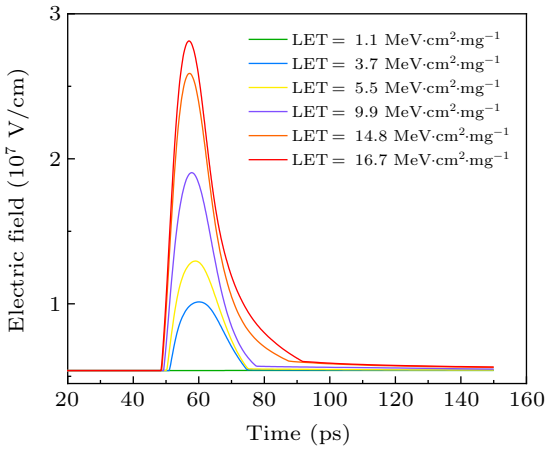


Fig. 9. Electric field caused by heavy ion incidence over time.

Using TCAD simulations, the variation of the ion-induced electric field peak within the SiC MOSFET under high voltage bias conditions was analyzed, as shown in Fig. 9. The sensitivity to SEEs involves considering the combined effects of the incident ion's LET and the reverse bias voltage. When studying the changes in the device's electrical characteristics due to heavy ion irradiation, it is generally assumed that breakdown is more likely to occur in regions where the electric field is concentrated.[2,23–25] The simulation results indicate that the ion-induced electric field peak inside the device increases sharply as the LET value rises. After 10 ps of irradiation with heavy ions having LET $>$ 10 MeV·cm^2·mg^{-1}, the peak electric field induced by high LET ions was significantly higher than that induced by the other four LET groups.

This increase in peak field results in a higher concentration of charge carriers accumulating at the device interface, thereby enhancing the electric field.

For different LET values, the simulation also examined the variation of ion-induced power density with respect to the device depth, as shown in Fig. 10. It has been demonstrated that while both high current density and high electric fields are of concern, it is the localized ion-induced effects that simultaneously elevate both, leading to significantly high localized power densities. This relationship is expressed by[26]

$$\text{Power density} = \boldsymbol{J} \cdot \boldsymbol{E}, \tag{1}$$

where power density (W/cm^3) is calculated as the dot product of current density (A/cm^2) and the electric field (V/cm).

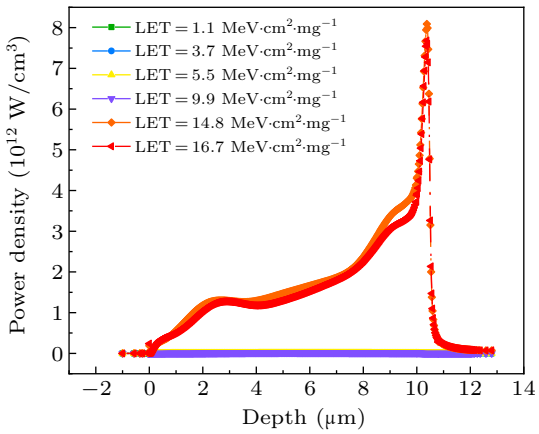


Fig. 10. Distribution of power density within the device as a function of depth.

Throughout the entire simulation process, the power density distribution within the SiC MOSFET increased with higher LET values. Under LET $>$ 10 MeV·cm^2·mg^{-1}, after ion irradiation, the power density along the ion trajectory inside the device reached approximately 7.5×10^{12} W/cm^3. In contrast, for ions with lower LET, the maximum power density along the ion trajectory inside the device was only about 5×10^9 W/cm^3.

The high electric field in the epitaxial layer, coupled with the ion-induced current, leads to excessively high power density, causing device breakdown and thermal runaway.[5] Therefore, the secondary ions which exhibit the LET distribution rather than a single energy, play a crucial role in the initiation of SEB. The secondary ions with LET $>$ 10 MeV·cm^2·mg^{-1}, as shown in Fig. 6(b), are the primary contributors to SEB in the device. All secondary ions that are shown to have sufficient range in the SiC and have a maximum LET value greater than 10 MeV·cm^2·mg^{-1} have the potential to cause catastrophic SEB of the SiC MOSFET, further supporting the device failure caused by the secondary ion. When a high-energy secondary ion strikes a SiC power MOSFET, it deposits energy in the semiconductor material, leading to the generation of a large number of electron–hole pairs along its track. The density of these generated charge carriers can be several orders of magnitude greater than the epitaxial doping concentration of the device. For instance, for an ion with a LET of 10 MeV·cm^2·mg^{-1}, the peak electron (or hole) density can reach 1×10^{19} cm^{-3}, which is significantly higher than the 5×10^{15} cm^{-3} epi doping in a 1200-V device. This high concentration of charge carriers effectively creates a low-resistance path between the source and drain regions of the MOSFET. Due to the creation of this conductive path by the ion strike, a high localized current can flow between the source and drain, particularly when the device is in the OFF-state and is subjected to a high voltage. The simulations described in the article model this scenario with the drain biased at a certain voltage and the source and gate grounded, which aligns with heavy-ion testing conditions. The ion track acts as a low-resistance channel allowing substantial current to flow. The ion strike also causes a redistribution of the internal electric fields within the power device, resulting in the formation of high electric field regions. The simultaneous presence of high current density and high electric fields in these localized areas leads to excessive localized power density dissipation. The TCAD simulations indicate that this power dissipation reaches its peak within about 10 ps following the ion strike.[26]

In summary, the microscopic physical processes of SEB in SiC power MOSFETs are characterized by the rapid generation of a large number of charge carriers due to an ion strike, the formation of a conductive path leading to high localized currents, the redistribution of electric fields creating high-field regions, and the resulting excessive localized power dissipation occurring within tens of picoseconds.

This simulation analysis demonstrates how the LET of secondary ions affects the power density distribution within the SiC MOSFET, providing valuable insights into the SEB that may occur during high-energy heavy ion exposure. The magnitude and location of this power dissipation, particularly at the epi and drain interface, are correlated with the SEB threshold of the devices. Devices with higher breakdown voltage ratings, achieved through thicker and more lightly doped epitaxial regions, exhibit a reduction in this ion-induced power dissipation, contributing to their increased SEB tolerance.

4. Conclusion and perspectives

This study highlights the critical role of high-energy O ions in inducing SEB in SiC MOSFETs through nuclear reactions that generate secondary ions with sufficient LET to penetrate the device's epitaxial layer. Our findings indicate that reverse bias voltage is a key factor in triggering SEB, with high voltages necessary for catastrophic failure. Simulations using GEANT4 and TCAD show that secondary ions with LET $>$

10 MeV·cm^2·mg^{-1} lead to significant ion-induced power densities within the device, causing thermal runaway and device breakdown. These insights deepen our understanding of the SEB mechanism and underscore the importance of secondary ions in the failure process. Further research should focus on exploring the impact of other low-LET heavy ions present in space radiation environments, such as those found in GCRs and SEPs, to better simulate the full range of radiation effects on SiC power devices. Additionally, design improvements, such as radiation-hardened SiC MOSFETs, could reduce the vulnerability of these devices to SEB. Testing in space or under simulated conditions is crucial to validate the findings and guide future space missions, ultimately enhancing the radiation resilience of SiC-based power electronics for space applications.

Acknowledgments

Project supported by the National Natural Science Foundation of China (Grant Nos. 12035019 and 62234013) and the National Key Research and Development Program of China (Grant Nos. 2023YFA1609000 and 2022YFB3604001).

We would like to thank the accelerator staff of the HIRFL.

References

[1] Ruddy F H, Dulloo A R, Seidel J G, Palmour J W and Singh R 2003 *Nucl. Instrum. Methods Phys. Res. A* **505** 159

[2] Singh R, Capell D C, Hefner A R, Lai J and Palmour J W 2002 *IEEE Trans. Electron Devices* **49** 2054

[3] Funaki T, Kimoto T and Hikihara T 2008 *IEEE Trans. Power Electron.* **23** 2602

[4] Ohshima T, Itoh H and Yoshikawa M 2001 *J. Appl. Phys.* **90** 3038

[5] Ball D R, Hutson J M, Javanainen A, Lauenstein J M, Galloway K F, Johnson R A, Alles M L, Sternberg A L, Sierawski B D, Witulski A F, Reed R A and Schrimpf R D 2020 *IEEE Trans. Nucl. Sci.* **67** 22

[6] Deki M, Makino T, Iwamoto N, Onoda S, Kojima K, Tomita T and Ohshima T 2014 *Nucl. Instrum. Methods Phys. Res. B* **319** 75

[7] Cao R, Wang K, Meng Y, Li L, Zhao L, Han D, Liu Y, Zheng S, Li H, Jiang Y, Zeng X and Xue Y 2023 *Chin. Phys. B* **32** 068502

[8] Tylka A J, Adams J H, Boberg P R, Brownstein B, Dietrich W F, Flueckiger E O, Petersen E L, Shea M A, Smart D F and Smith E C 1997 *IEEE Trans. Nucl. Sci.* **44** 2150

[9] Zhang H, Guo H, Lei Z, Peng C, Zhang Z, Chen Z, Sun C, He Y, Zhang F, Pan X, Zhong X and Ouyang X 2023 *Chin. Phys. B* **32** 028504

[10] Martinella C, Natzke P, Alia R G, Kadi Y, Niskanen K, Rossi M, Jaatinen J, Kettunen H, Tsibizov A, Grossner U and Javanainen A 2022 *Microelectron. Reliab.* **128** 114423

[11] Lauenstein J M, Casey M C, Ladbury R L, Kim H S, Phan A M and Topper A D 2021 *IEEE Int. Reliab. Phys. Symp. (IRPS)* 1

[12] Burigo L N, Pshenichnov I A, Mishustin I N and Bleicher M 2014 *J. Phys.: Conf. Ser.* **503** 012021

[13] Zhang H, Guo H, Zhang F, Lei Z, Pan X, Liu Y, Gu Z, Ju A, Zhong X and Ouyang X 2021 *Microelectron. Reliab.* **124** 114329

[14] Li X, Jiang W, Wang Y, Zhang H, Peng C, Zhang X, Liang X, Fu W, Zhang Z, Lei Z, Ma T and Yang J Y 2024 *Appl. Phys. Lett.* **125** 092101

[15] Siddiqui A, Hallén A and Usman M 2023 *Phys. Status Solidi A* **220** 2300300

[16] Zhang H, Guo H X, Lei Z F, Peng C, Ma W Y, Wang D, Sun C H, Zhang F Q, Zhang Z G, Yang Y, Lv W, Wang Z M, Zhong X L and Ouyang X P 2023 *Chin. Phys. B* **32** 108503

[17] Kuboyama S, Matsuda S, Kanno T and Hirose T 1994 *IEEE Trans. Nucl. Sci.* **41** 2210

[18] Ziegler J F, Ziegler M D and Biersack J P 2010 *Nucl. Instrum. Methods Phys. Res. B* **268** 1818

[19] Martinella C, Natzke P, Alia R G, Kadi Y, Niskanen K, Rossi M, Jaatinen J, Kettunen H, Tsibizov A, Grossner U and Javanainen A 2022 *Microelectron. Reliab.* **128** 114423

[20] Witulski A F, Ball D R, Galloway K F, Javanainen A, Lauenstein J M, Sternberg A L and Schrimpf R D 2018 *IEEE Trans. Nucl. Sci.* **65** 1951

[21] Agostinelli S, *et al*. 2003 *Nucl. Instrum. Methods Phys. Res. A* **506** 250

[22] Allison J, *et al*. 2016 *Nucl. Instrum. Methods Phys. Res. A* **835** 186

[23] Li M B, Cao F, Hu H F, Li X J, Yang J Q and Wang Y 2021 *IEEE J. Electron Devices Soc.* **9** 591

[24] Makino T, Deki M, Iwamoto N, Onoda S, Hoshino N, Tsuchida H, Hirao T and Ohshima T 2013 *IEEE Trans. Nucl. Sci.* **60** 2647

[25] Dong X, Huang M, Ma Y, Fu C, He M, Yang Z, Li Y and Gong M 2024 *IEEE Trans. Nucl. Sci.* **71** 2252

[26] Ball D R, Galloway K F, Johnson R A, Alles M L, Sternberg A L, Witulski A F, Reed R A, Schrimpf R D, Hutson J M and Lauenstein J M 2021 *IEEE Trans. Nucl. Sci.* **68** 1430